Protonation of Histidine-132 Promotes Oligomerization of the Channel-Forming Toxin Aerolysin†

J. Thomas Buckley,‡ H. Ulrich Wilmsen,§ Claire Lesieur,|| Angela Schulze,‡ Franc Pattus,⊥ Michael W. Parker,# and F. Gisou van der Goot*,||

Department of Biochemistry and Microbiology, University of Victoria, Box 3055, Victoria, British Columbia, Canada V8W 3P6, ESBS, UPR 9050, CNRS, Rue Sébastien Brant, 67400 Illkirch, France, Institüt für Biophysik, Johanes Kepler University Linz, 4040 Linz-Auhof, Austria, St. Vincent's Institute of Medical Research, 41 Victoria Parade, Fitzroy, Victoria, 3065, Australia, and Département de Biochimie, Université de Genève, 30 quai E. Ansermet, 1211 Genève, Switzerland

Received August 28, 1995; Revised Manuscript Received October 13, 1995⊗

ABSTRACT: Aerolysin is a bacterial toxin that binds to a receptor on eukaryotic cells and oligomerizes to form stable, SDS-resistant, noncovalent oligomers that insert into the plasma membrane and produce well-defined channels. Little is known about the mechanisms controlling this process. Here we show that the protonation of a single histidine is required for oligomerization of aerolysin in solution. First we have investigated the effect of pH on the activity of aerolysin. The toxin's ability to disrupt human erythrocytes declined as the pH increased above 7.4. Experiments with receptor-free planar lipid bilayers demonstrated that the rate at which aerolysin formed channels also decreased with increasing pH, although the conductance of preexisting channels was not affected. The reduction in the rate of channel formation was shown to be due to a decrease in the toxin's ability to oligomerize. Our data indicate that the pH effect on activity is due to the deprotonation of a single residue rather than a global effect of pH on the protein. In agreement with our previous site-directed mutagenesis studies, His-132 is most likely to be the target of this pH effect. This conclusion was reinforced by the fact that we could shift the pH dependence of the activity to lower pH values by mutating Asp-139, a residue less than 3 Å away from His-132 and likely to contribute to the unusually high pK_a of this histidine.

Aerolysin is a prototype of a group of pore-forming toxins that contain a high percentage of β-sheet structure and must oligomerize in order to insert into the membranes of target cells and generate defined channels [for a review, see Buckley (1992) and van der Goot *et al.* (1994b)]. Other members of the group include the α toxins from *Staphylococcus aureus* and *Clostridium septicum*, the protective antigen of anthrax toxin, and some of the oxygen-labile toxins (Bhakdi & Tranum-Jensen, 1991; Ballard *et al.*, 1993; Boulnois *et al.*, 1991; Milne *et al.*, 1994). *Aeromonas* species secrete aerolysin as a 52 kDa precursor that is activated by proteolytic removal of about 40 amino acids from the C-terminus (Howard & Buckley, 1985; van der Goot *et al.*, 1992, 1994a). The toxin is concentrated on the surface of the target cell by binding to a specific receptor (Gruber *et al.*, 1994). Activation and concentration lead to oligomerization, and this is a prerequisite for channel formation, as the oligomer not only is the insertion-competent form of the toxin but also generates the channel (Buckley, 1992; van der Goot *et al.*, 1994b).

Our knowledge of the mechanism of action of aerolysin has increased significantly over the past years, but despite the fact that the crystal structure has recently been solved (Parker *et al.*, 1994), the molecular details of receptor binding, oligomerization, and channel formation are poorly understood. Using site-directed mutagenesis, we have identified several residues in domain 2 [see Parker *et al.* (1994)] of the toxin that appear to be important for oligomerization. Both tryptophan 371 and tryptophan 373 are part of an aromatic bowl in this domain, and when either of them is replaced with leucine, the toxin's ability to oligomerize is increased (van der Goot *et al.*, 1993b). When His-132, which is in the same region, is replaced with asparagine, the toxin can no longer oligomerize in solution (Green & Buckley, 1990; Wilmsen *et al.*, 1991). In the present paper we study the effect of changes in pH on channel formation, and we provide more detailed evidence that the region around His-132 is critical in the oligomerization process.

MATERIALS AND METHODS

Materials. Diethyl pyrocarbonate (DEPC)[1] and asolectin were purchased from Sigma (St. Louis), and 8-anilino-1-naphthalenesulfonate (ANS) was obtained from Fluka. Wild-type and variant proaerolysins were purified as described previously (Buckley, 1990). Concentrations were calculated based on an absorbance of 2.5 at 280 nm for pure 1 mg/mL solutions of toxin or protoxin (van der Goot *et al.*, 1994a).

† This work has been supported by grants from the National Sciences and Engineering Research Council of Canada (J.T.B.), the National Health and Medical Research Council of Australia (M.W.P.), and the Swiss National Science Foundation (F.G.v.d.G.).

‡ University of Victoria.
§ Johanes Kepler University Linz.
|| Université de Genéve.
⊥ CNRS.
St. Vincent's Institute of Medical Research.

⊗ Abstract published in *Advance ACS Abstracts,* December 1, 1995.

[1] Abbreviations: ANS, 8-anilino-1-naphthalenesulfonate; UV CD, near-ultraviolet circular dichroism; DEPC, diethyl pyrocarbonate; EPPS, *N*-(2-hydroxyethyl)piperazine-*N*′-3-propanesulfonic acid; HEPES, *N*-(2-hydroxyethyl)piperazine-*N*′-2-ethanesulfonic acid; MES, 2-(*N*-morpholino)ethanesulfonic acid; PBS, phosphate saline buffer, pH 7.4; H132N, toxin in which His-132 has been mutated to Asn; D139N, toxin in which Asp-139 has been mutated to Asn; H332N, toxin in which His-332 has been mutated to Asn.

0006-2960/95/0434-16450$09.00/0

Site-Directed Mutagenesis. Mutagenesis was performed on the 715 bp *Hin*dIII−*Hin*cII of aerA in the phagemid pTZ18U according to the manufacturer's instructions (Bio-Rad). Changes were confirmed by DNA sequencing using Sequenase version 2 and materials and procedures provided by U. S. Biochemicals. Once a clone was identified, the DNA was inserted in-frame with the rest of aerA in pTZ18U. Then the entire 1.7 bp aerA gene was cloned into pMMB66HE and transferred to the *Aeromonas salmonicida* by conjugative mating as described in Wong *et al.* (1990).

Hemolytic Activity. Hemolytic titers were obtained as previously described (Howard & Buckley, 1982). Values are expressed as the $\log_2$ of the highest dilution that results in complete cell lysis. All buffers contained 150 mM NaCl and 10 mM buffer. *N*-(2-Hydroxyethyl)piperazine-*N*′-[2-ethanesulfonic acid (HEPES) was used between pH 7.4 and 8 and Tris-HCl at pH 8.5 and 9.

The rate of hemolysis after DEPC treatment (see below) was determined by measuring the change in the optical density of a suspension of human erythrocytes [0.4 mL of packed cells/100 mL of phosphate saline buffer (PBS)] at 600 nm as a function of time at 37 °C after addition of the modified or control toxin.

Lipid Bilayer Experiments. Planar lipid bilayers were formed by apposition of two lipid monolayers in the aperture (diameter 180 μm) of a 5 μm thick Teflon septum as previously described (Wilmsen *et al.*, 1990). The solutions used contained 1 M NaCl, 5 mM $CaCl_2$, and 20 mM of one of the following buffers: 2-(*N*-morpholino)ethanesulfonic acid (MES) in the 6.0−7.0 pH range, HEPES in the 7.1−8.0 pH range, and Tris-HCl for pH values above 8.0. The membrane current for recording multichannel incorporation curves was amplified using a I-V converter with an operational amplifier (Burr Brown 3528) and feedback resistors ranging from 10^7 to 1.5×10^8 W. The *trans* compartment was connected to the I-V converter and held at virtual ground potential. The sign of the membrane potential refers to the *cis* side of the membrane. Aerolysin was added to the solution on the *cis* side of the bilayer (final concentration of 2 μg/mL) with vigorous stirring.

Light Scattering and ANS Binding Experiments. Experiments were performed with an SLM 8000 spectrofluorometer (Urbana, IL). For light scattering experiments, the excitation wavelength was 450 nm with 8 nm slit widths. For ANS binding experiments, excitation and emission wavelengths were 380 and 480 nm, respectively, with spectral bandwidths of 4 nm. The final ANS concentration was 5 μM. In both types of experiments, proaerolysin was diluted to a final concentration of 0.16 mg/mL in 150 mM NaCl, 20 mM buffer adjusted to the desired pH. HEPES was used between pH 7 and 7.8 and *N*-(2-hydroxyethyl)piperazine-*N*′-3-propanesulfonic acid (EPPS) between pH 8 and 8.8. Proaerolysin was activated by addition of trypsin to a final concentration of 1 μg/mL.

Circular Dichroism (CD). Circular dichroic measurements were made between 250 and 325 nm at room temperature in a Jasco 600 spectrometer using quartz cells of 1 cm path length. The proaerolysin concentration was 0.5−0.6 mg/mL in 150 mM NaCl, 20 mM HEPES, pH 7.4.

Stability of Wild-Type and Variant Proaerolysins as a Function of Urea Concentration. The maximum emission of tryptophan residues was used as a probe of the protein's conformation (van der Goot *et al.*, 1993a). Fluorescence measurements were made using a Perkin Elmer LS-5B spectrofluorometer. The excitation wavelength was 295 nm, and the slit width was 5 nm for the excitation and 2.5 nm for the emission. Experiments were done in the presence of 150 mM NaCl and 20 mM buffer. MES was used at pH 5.5, HEPES at pHs 7.4 and 7.8, EPPS at pH 8.4, and borate buffer at pH 9.4 at a proaerolysin concentration of 25 μg/mL. Samples were incubated with urea for 120 min before spectra were taken. For each recorded spectrum, the Raman contribution of water was removed by subtraction of a buffer blank.

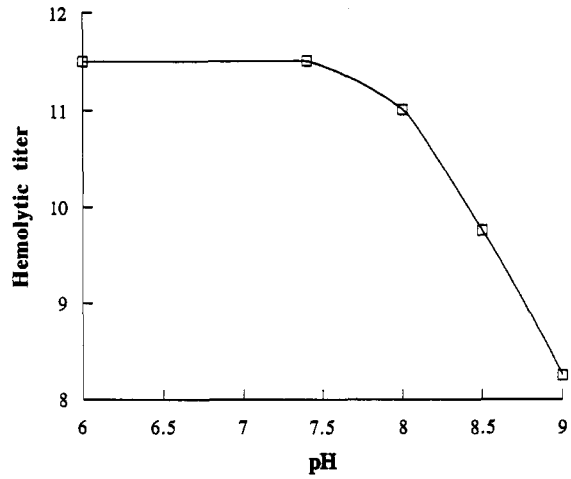

FIGURE 1: Hemolytic activity of wild-type aerolysin as a function of pH. Titers are expressed as the $\log_2$ of the highest dilution resulting in complete hemolysis. Results are the means of three identical experiments.

Modification of Wild-Type and D139N Aerolysins by DEPC. Wild-type or D139N proaerolysin in 20 mM HEPES, 150 mM NaCl, pH 7.4, was activated with trypsin (4 μg/mL) for 10 min at room temperature. A 5-fold excess of trypsin inhibitor was then added. Aerolysin thus obtained was diluted 5-fold in a solution containing 50 mM buffer, 150 mM NaCl at the desired pH. The buffers used were as follows: sodium acetate from pH 4 to 5.5; sodium phosphate from pH 6 to 8; and tricine above pH 8. Exact pH values were measured after dilution. DEPC was added to a final concentration of 0.2 mM (Miles, 1977). Fresh stock solutions of DEPC were prepared in anhydrous ethanol immediately before use. The actual DEPC concentration in the stock solution was determined by its reaction with free imidazole (Miles, 1977). The modified toxin was tested for hemolytic activity. A sample of aerolysin was treated with ethanol as a control at each pH.

RESULTS

pH Dependence of the Hemolytic Activity. As a first step, we measured the hemolytic activity of the toxin as a function of pH using human erythrocytes. As illustrated in Figure 1, activity declined rapidly as the pH was raised above 8, and at pH 8.5, it was 4 times lower than at pH 7.4 (corresponding to a decrease of 2 in the titer).

pH Dependence of the Rate of Channel Formation. Changes in several of the steps occurring during channel formation by aerolysin could account for the inhibition observed in Figure 1. In order to eliminate any possible contribution of interactions between the toxin and its cellular receptor, we measured the pH dependence of channel formation in asolectin lipid bilayers. As shown in Figure

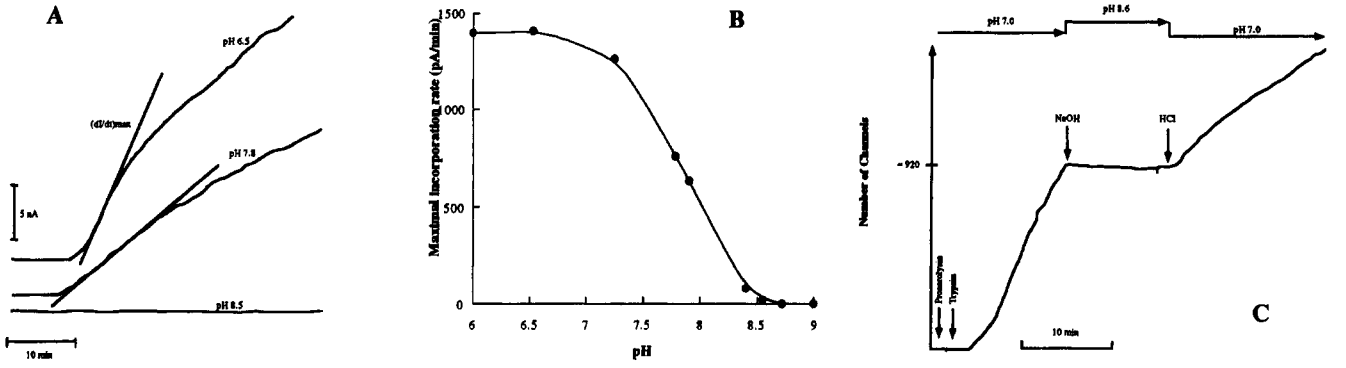

FIGURE 2: pH dependence of channel formation in asolectin planar lipid bilayers by aerolysin. (A) Kinetics of multichannel incorporation curves by mature aerolysin were measured at various pH values. The applied voltage was +50 mV. The final aerolysin concentration was 2 μg/mL. (B) For each pH value, the maximal slope of the increase in transmembrane current, $J_{max} = (dI/dt)_{max}$, was determined. Each data point represents the mean of 3−8 experiments. (C) Kinetics of channel formation were measured at pH 7.2. After 10 min, the *cis* pH was increased to 8.6 by addition of 1 M Tris base. After an additional 15 min, the pH was dropped again by addition of 1 M acetic acid.

2A, the rate of transmembrane current increase was highest at pH 6.5, and no transmembrane current could be detected at pH 8.5. A plot of the maximal slope of the transmembrane current increase as a function of time [$J_{max} = (dI/dt)_{max}$] against pH revealed a midpoint transition around pH 7.8 (Figure 2B).

The changes recorded in Figure 2A,B could also have been due to a decline in single-channel conductance with increasing pH. This was ruled out by the results of an experiment in which changes in the conductance of existing channels were measured. Approximately 900 aerolysin channels were allowed to form over a time period of 10 min at pH 7.0. After raising the pH of the *cis* compartment to 8.6 with 1 M Tris base, the increase in transmembrane current completely stopped (Figure 2C). Since the current then remained constant and did not decline, we can conclude that the high pH did not reduce the conductance of existing channels. After an additional time period of 15 min, the pH was returned to 7.0 with 1 M acetic acid. Then the transmembrane current resumed, indicating that no new channels were incorporated and demonstrating that the inhibitory effects of elevated pH on channel formation were fully reversible.

Effect of pH on the Ability of Wild-Type Aerolysin To Oligomerize in Vitro. We have previously shown that oligomerization of aerolysin in solution can be measured by following the accompanying increase either in light scattering or in binding of the hydrophobic probe ANS (van der Goot *et al.*, 1992, 1993b). As illustrated in Figure 3, the kinetics of oligomerization measured using either method showed a clear pH dependence (Figure 3), which correlated well with the effects we observed on channel formation in artificial lipid bilayers (also plotted in Figure 3). This observation shows that channel formation did not occur because the toxin was unable to oligomerize.

Effect of pH on the Structure and Stability of Proaerolysin. The steepness of the inhibition curve in Figure 3 suggests that inhibition of oligomerization might be due to the deprotonation of a single residue with an apparent pK_a of about 7.8. Alternatively, the reduced ability to oligomerize at basic pH may also be due to an overall pH effect either on the structure or on the stability of the protein. To test the validity of this latter proposal, we measured the near-ultraviolet circular dichroism (UV CD) spectrum of proaerolysin between pH 4 and 8.5, as the near-UV CD spectrum is very sensitive to small changes in structure (van der Goot *et al.*, 1992). The spectrum was unchanged over this pH range (data not shown), indicating that major changes in the structure of proaerolysin cannot account for the observed effects of pH on oligomerization.

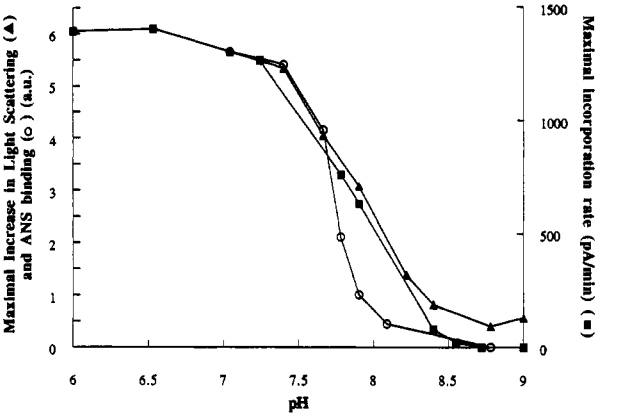

FIGURE 3: Effect of pH on the initial rate of oligomerization of aerolysin in solution. Comparison with the effect of pH on the initial rates of channel formation in a lipid bilayers. Oligomerization of aerolysin followed by measuring either the increase in scattered light or the increase in fluorescence of the hydrophobic probe ANS upon activation of proaerolysin with trypsin. The initial slopes of increase in light scattering (▲) or ANS fluorescence (○) were plotted as a function of pH. The maximal slopes of increase in transmembrane current are those plotted in Figure 2 (■).

The influence of pH on the conformational stability of the protoxin was then studied by measuring the sensitivity to urea denaturation. The maximal emission of tryptophans was chosen as a comparison parameter (van der Goot *et al.*, 1993a). Lowering the pH to 5.5 had no measurable effect on the stability of the protoxin. However, increasing the pH led to noticeable destabilization. The midpoint of unfolding occurred in 4 M urea at pH 7.4, 3.75 M urea at pH 7.8, 3 M urea at pH 8.4, and 2.7 M urea at pH 9.4.

Evidence That Deprotonation of His-132 Decreases the Ability of Aerolysin to Oligomerize. If inhibition by pH was due to deprotonation of a single residue, then the imidazole ring of His-132 would be the most likely candidate. Indeed, His-132 is the only histidine essential for oligomerization (Green & Buckley, 1990). We have previously shown that replacement of His-132 with Asn reduces the oligomerization capacity on the surface of erythrocytes as compared to wild type (Green & Buckley, 1990), and blocks both oligomerization in solution and channel formation in planar lipid

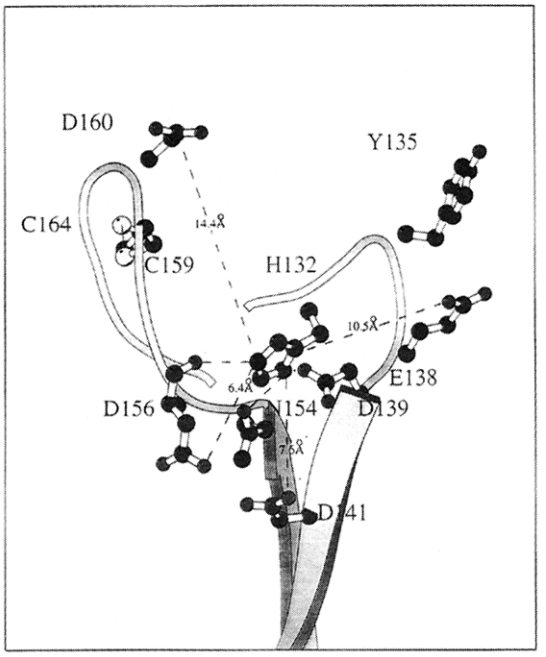

FIGURE 4: Three-dimensional environment of His-132. Schematic representation of His-132 surrounded by the five carboxyl groups Glu-138, Asp-139, Asp-141, Asp-156, and Asp-160 in the crystal structure (Parker *et al.*, 1994). The figure was produced with the program MOLSCRIPT (Kraulis, 1991).

bilayers (Wilmsen *et al.*, 1991). However, the pK_a of His-132 would have to be unusually high since the pK_a of the imidazole group is around 6.3 under normal conditions (Antosiewicz *et al.*, 1994), and we observed 50% inhibition of oligomerization at pH 7.8 (Figure 3). Examination of the environment of His-132 in the three-dimensional crystal structure of the toxin suggested that its pK_a may be strongly affected by neighboring residues (Figure 4). Five carboxyl groups are nearby, contributed by Glu-138 (10.5 Å away), Asp-139 (3 Å), Asp-141 (7.6 Å), Asp-156 (6.4 Å), and Asp-160 (14.4 Å) (Parker *et al.*, 1994), and they are expected to significantly increase the effective pK_a of the histidine. Because of the size of aerolysin we were unable to titrate histidine residues by NMR (unpublished results). In addition, we could not reliably calculate the pK_a of His-132 based on its position in the three-dimensional structure of the protein (Gilson & Honig, 1987). His-132 forms a hydrogen bond with a neighboring Asp-139, and as a result the effective charge of the aspartic acid is reduced to an unknown extent. As no charge could be assigned to Asp-139, the algorithms established by Gilson and Honig (1987) could not be applied.

In order to get an indication of the pK_a of His-132, we took advantage of its reaction with DEPC, which Garland and Buckley (1988) have shown to inhibit oligomerization when used at pH 7.4. Its likely target is His-132 as this is the only histidine essential for oligomerization (Green & Buckley, 1990). Since DEPC modifies only unprotonated histidines (Miles, 1977), the pH dependence of inactivation should reflect the pK_a of the affected histidine.

Although DEPC preferentially reacts with histidines (Davis *et al.*, 1994; Miles, 1977; Zhang *et al.*, 1992), we first investigated whether no other essential amino acids in aerolysin were also modified as DEPC has been reported to occasionally react with lysines and cysteines, and more rarely with tyrosines. The four cysteines of aerolysin form two disulfide bridges (Parker *et al.*, 1994; and unpublished

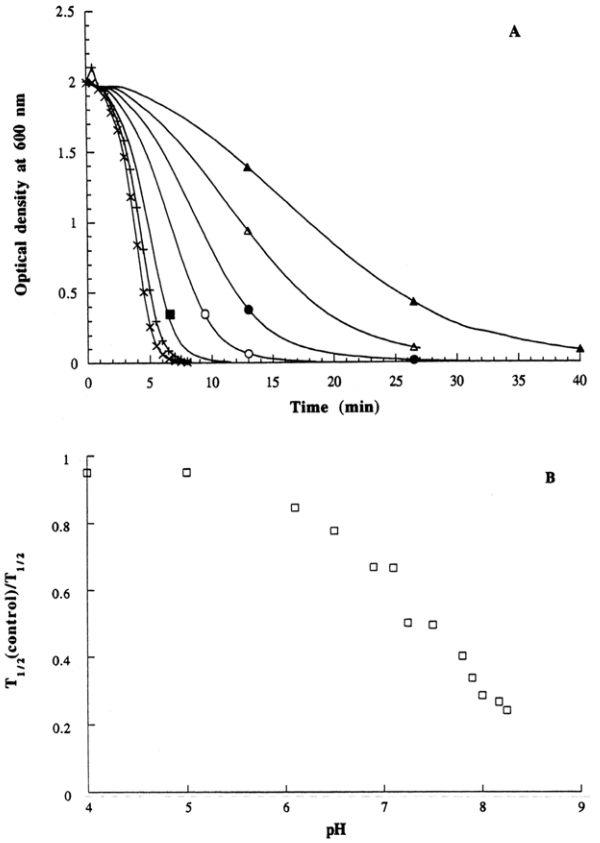

FIGURE 5: pH-dependent inactivation of wild-type aerolysin by DEPC. Wild-type aerolysin was modified by 0.2 mM DEPC at various pH values, and the hemolytic activity was then assessed. (A) Kinetics of hemolysis were followed by measuring the decrease in the optical density of a 0.4% human erythrocyte suspension in PBS (pH 7.4) upon addition of modified aerolysin. Control pH 5 (×); DEPC-treated: pH 5 (+) ; pH 6.5 (■); pH 7.1 (○); pH 7.5 (●); pH 7.9 (△); pH 8.25 (▲). The aerolysin concentration during the hemolysis experiments was 20 nM for wild type. (B) The time needed to reach half of the initial OD was determined for each pH, both for aerolysin treated with DEPC [$t_{1/2}$(DEPC)] and for control aerolysin treated with anhydrous ethanol [$t_{1/2}$(control)]. The ratio $t_{1/2}$(control)/$t_{1/2}$(DEPC) was plotted as a function of pH.

results) and therefore are not accessible for reaction. Lysine modification with DEPC is irreversible, whereas single N-carboxyethylation of histidines can be reversed by treating the modified protein with hydroxylamine at neutral pH (Miles, 1977). When aerolysin was labeled with 0.2 mM DEPC at pH 7.4 for 15 min, its activity was reduced to 25% of the control. Treatment for 18 h with 0.3 M hydroxylamine, pH 7 at room temperature in the dark followed by dialysis against PBS at 4 °C restored the initial hemolytic titer, thus excluding an effect on essential lysine residues.

We then studied the effect of pH on the inactivation of the toxin. Aerolysin was therefore activated with trypsin for 10 min, and then trypsin inhibitor was added. The sample was diluted into a buffer at the required pH and treated with 0.2 mM DEPC (diluted from a stock in ethanol) for 15 min. For each pH, a control aerolysin sample was treated with a corresponding amount of ethanol alone. The kinetics of hemolysis were then measured at pH 7.4 as described under Materials and Methods. No significant effects on the rate of hemolysis could be observed when aerolysin modified with DEPC at pHs below 6.0 was used. However, as illustrated in Figure 5A, the rate of hemolysis decreased in the presence of toxin treated with DEPC at progressively

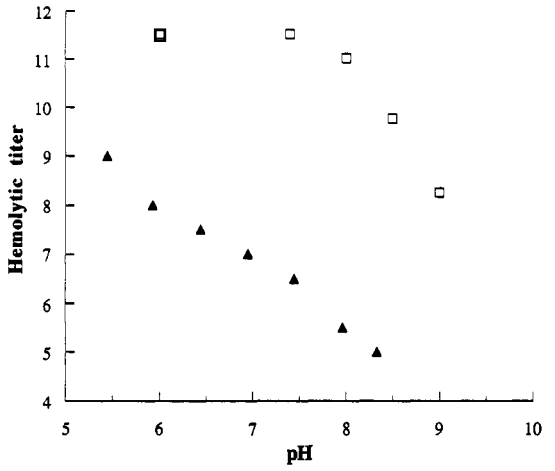

FIGURE 6: Comparison of the effect of pH on the hemolytic activity of wild-type and D139N aerolysin. Titers are expressed as the $\log_2$ of the highest dilution resulting in complete hemolysis. Results are the means of three identical experiments. The wild-type (□) values are those plotted in Figure 1. D139N (▲).

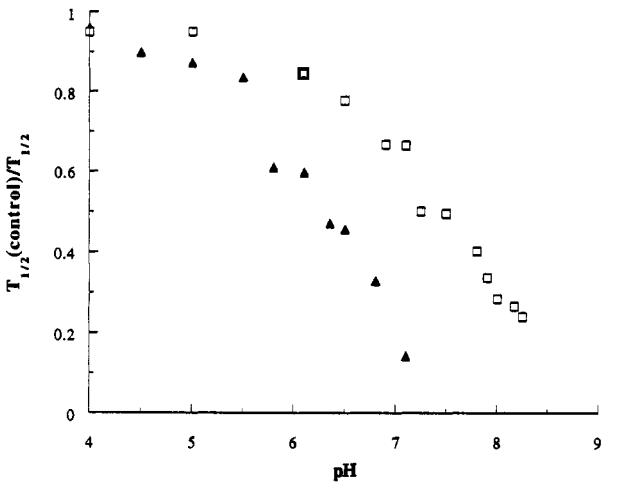

FIGURE 7: Comparison of the effect of DEPC modification on the hemolytic activity of wild-type and D139N aerolysin. As in Figure 5B, the ratio $t_{1/2}$(control)/$t_{1/2}$(DEPC) obtained for D139N (▲) was plotted as a function of pH. The wild-type (□) values are those plotted in Figure 5B. The concentration of D139N aerolysin during the hemolysis experiments was 200 nM.

higher pHs. The time required to reach half of the initial optical density ($t_{1/2}$) was determined at each pH and compared to corresponding controls. In Figure 5B, the ratio $t_{1/2}$(control)/$t_{1/2}$(DEPC) has been plotted as a function of pH. The results, which are reminiscent of a titration curve, indicate that DEPC modifies a residue (or residues) with a pK_a between 7 and 8 which is likely to be His-132.

The modification of His-132 by DEPC at higher pH values is most likely due to the deprotonation of this residue rather than to a change in accessibility as a consequence of a pH-induced conformation change. According to the crystal structure, His-132 is exposed at the surface of the protein even at low pH, and therefore expected to be accessible to DEPC. Moreover, no change in conformation could be detected between pH 6 and 8 as witnessed by near-UV CD spectroscopy (see below). As the region surrounding His-132 is very rich in aromatic residues, a conformational change in this region would have led to an alteration of the near-UV CD spectrum.

Consequences of Altering the Environment of His-132. In order to determine if the environment around His-132 affects the pH dependence of the toxin's activity, we replaced Asp-139, the nearest acidic residue (only 3 Å away), with asparagine, anticipating that the pK_a of His-132 would be lowered. The near-UV CD spectrum of D139N proaerolysin was very similar to that of the wild-type protein (data not shown), an indication that this mutation did not significantly affect the rigidity of the tertiary interactions in the protein. The results in Figure 6 show that hemolytic activity is inhibited at a lower pH than with wild-type aerolysin, thus supporting the view that deprotonation of His-132 reduces the toxin's ability to form a channel.

The effects of DEPC modification on hemolysis by D139N aerolysin were also analyzed. As for wild type, increasing the pH at which the reaction was performed led to increasing inhibition of the hemolytic activity (Figure 7). However, for D139N, inhibition occurred at about 1 pH unit lower than for the wild-type toxin, indicating that the mutation did decrease the effective pK_a of His-132. As Asp-139 is more than 13 Å from His-107 and 25 Å from His-332, interactions

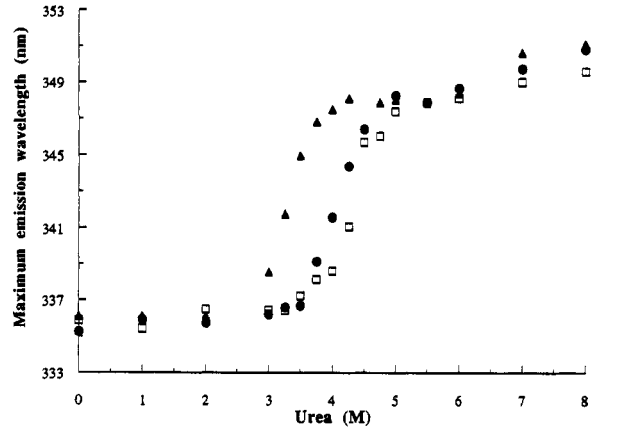

FIGURE 8: Effect of mutating His-132 to Asn and Asp-139 to Asn on the stability of proaerolysin. Denaturation by urea as determined by the change in maximum emission wavelength of tryptophans was measured for both H132N and D139N proaerolysin variants. Wild type, □; H132N, ●; D139N, ▲.

with these residues are unlikely. In any case, neither of these histidines is required for oligomerization (Green & Buckley, 1990).

As shown in Figure 8, replacing Asp-139 with Asn had a somewhat destabilizing effect on the structure of proaerolysin, whereas changing His-132 to asparagine did not alter the stability of the protoxin. Experiments measuring spontaneous oligomerization of D139N lead to the striking observation that D139N seemed unable to form oligomers in solution or in the presence of liposomes, as monitored by SDS–PAGE gel electrophoresis as well as by measuring binding ANS upon activation. D139N was, however, able to oligomerize at the surface of erythrocyte membranes as shown by Western Blot analysis (data not shown), suggesting that this variant of aerolysin might require the presence of a receptor for a yet unknown reason.

DISCUSSION

Taken together, the results of these experiments lead to the conclusion that the deprotonation of His-132 decreases

the channel-forming activity of aerolysin by reducing the toxin's ability to oligomerize. Recently, Gibbons and Horowitz (1995) made a comparable observation with GroEL. They found that protonation of His-401 leads to exposure of hydrophobic surfaces on the chaperonin that increased the stability of its interaction with an unfolded protein.

It seems more likely that His-132 affects a structurally sensitive region in aerolysin rather than that the residue plays a solitary role in oligomerization. According to the crystal structure, this residue not only interacts with the carboxyl side chain of Asp-139 and the side chain of Asn-154 but, in the protonated form, it most likely forms a hydrogen bond with the side chain carbonyl of Asp-156. The relative locations of these three amino acids suggest that Asp-139 positions the aromatic side chain of His-132 to optimize its interaction with Asp 156. This is of particular interest since Asp-156 is part of a large flexible loop running from amino acids 153−168 that we have identified as being important for the function of the toxin (unpublished data). This loop contains a disulfide bond which bridges Cys-159 and Cys-164 (Parker *et al.*, 1994; and unpublished data). Although only four amino acids separate the cysteines, this bridge has a stabilizing effect on the structure of the protein (van der Goot and Buckley, unpublished results). Moreover, a variant in which Cys-159 was changed to serine was found to oligomerize less efficiently than wild type (Buckley, unpublished results).

One could also imagine that His-132 itself is important for oligomerization, for example, if it were situated at an important point on the monomer−monomer interface in the oligomer. However, according to the current model of the oligomer proposed by Parker *et al.* (1994 and submitted), this does not seem to be the case. It is also possible that His-132 affects oligomerization indirectly by influencing the stability of the dimer. It is in close proximity to residues such as Tyr-135 and Glu-138 which are involved in monomer−monomer contacts both in the dimer and in the oligomer (Parker et al., 1994). It is worth noting that although the H132N variant is unable to generate oligomers in solution, it can participate in the formation of SDS-stable heterooligomers with wild type (data not shown). Although the significance of this remains to be elucidated, it appears to exclude an effect of His-132 on oligomer stability and therefore suggests that the region surrounding His-132 might be important at the onset of oligomerization, for example, acting as a nucleation site to trigger the process.

ACKNOWLEDGMENT

M.W.P. is a Wellcome Australian Senior Research Fellow. We thank Dr. P. Graber for giving us access to the circular dichroism spectrophotomer of the Glaxo Institute (Geneva).

REFERENCES

Antosiewicz, J., McCammon, J. A., & Gilson, M. K. (1994) *J. Mol. Biol. 238*, 415−436.
Ballard, J., Sokolov, Y., Yuan, W.-L., Kagan, B. L., & Tweten, R. K. (1993) *Mol. Microbiol. 10*, 627−634.
Bhakdi, S., & Tranum-Jensen, J. (1991) *Microbiol. Rev. 55*, 733−751.
Boulnois, G. J., Paton, J. C., Mitchell, T. J., & Andrew, P. W. (1991) *Mol. Microbiol. 5*, 2611−2616.
Buckley, J. T. (1990) *Biochem. Cell Biol. 68*, 221−224.
Buckley, J. T. (1992) *FEBS Lett. 307*, 30−33.
Davis, J., Zhou, M.-M., & Van Etten, R. (1994) *Biochemistry 33*, 1278−1286.
Garland, W. J., & Buckley, J. T. (1988) *Infect. Immun. 56*, 1249−1253.
Gibbons, D. L., & Horowitz, P. M. (1995) *J. Biol. Chem. 270*, 7335−7340.
Gilson, M., & Honig, B. (1987) *Nature 330*, 84−87.
Green, M. J., & Buckley, J. T. (1990) *Biochemistry 29*, 2177−2180.
Gruber, H. J., Wilmsen, H. U., Cowell, S., Schindler, H., & Buckley, J. T. (1994) *Mol. Microbiol. 14*, 1093−1101.
Howard, S. P., & Buckley, J. T. (1982) *Biochemistry 21*, 1662−1667.
Howard, S. P., & Buckley, J. T. (1985) *J. Bacteriol. 163*, 336−340.
Kraulis, J. P. (1991) *J. Appl. Crystallogr. 24*, 946−950.
Miles, W. (1977) *Methods Enzymol. 47*, 431−442.
Milne, J. C., Furlong, D., Hanna, P. C., Wall, J. S., & Collier, R. J. (1994) *J. Biol. Chem. 269*, 20607−20612.
Parker, M. W., Buckley, J. T., Postma, J. P. M., Tucker, A. D., Leonard, K., Pattus, F., & Tsernoglou, D. (1994) *Nature 367*, 292−295.
van der Goot, F. G., Lakey, J. H., Pattus, F., Kay, C. M., Sorokine, O., Van Dorsselaer, A., & Buckley, T. (1992) *Biochemistry 31*, 8566−8570.
van der Goot, F., Ausio, J., Wong, K., Pattus, F., & Buckley, J. (1993a) *J. Biol. Chem. 268*, 18272−18279.
van der Goot, F. G., Wong, K. R., Pattus, F., & Buckley, J. T. (1993b) *Biochemistry 32*, 2636−2642.
van der Goot, F. G., Hardie, K. R., Parker, M. W., & Buckley, J. T. (1994a) *J. Biol. Chem. 269*, 30496−30501.
van der Goot, F. G., Parker, M., Pattus, F., & Buckley, J. T. (1994b) *Toxicology* 87, 19−28
Wilmsen, H. U., Pattus, F., & Buckley, J. T. (1990) *J. Memb. Biol. 115*, 71−81.
Wilmsen, H. U., Buckley, J. T., & Pattus, F. (1991) *Mol. Microbiol. 5*, 2745−2751.
Wong, K. R., McLean, D. M., & Buckley, J. T. (1990) *J. Bacteriol. 172*, 372−376.
Zhang, Z.-Y., Davis, J., & Van Etten, R. (1992) *Biochemistry 31*, 1701−1711.

BI952041R